Research Article

A LES Study on Passive Mixing in Supersonic Shear Layer Flows Considering Effects of Baffle Configuration

Ren Zhao-Xin and Wang Bing

School of Aerospace, Tsinghua University, Beijing 100084, China

Correspondence should be addressed to Wang Bing; wbing@tsinghua.edu.cn

Under the background of dual combustor ramjet (DCR), a numerical investigation of supersonic mixing layer was launched, focused on the mixing enhancement method of applying baffles with different geometric configurations. Large eddy simulation with high order schemes, containing a fifth-order hybrid WENO compact scheme for the convective flux and sixth-order compact one for the viscous flux, was utilized to numerically study the development of the supersonic mixing layer. The supersonic cavity flow was simulated and the cavity configuration could influence the mixing characteristics, since the impingement process of large scale structures formed inside the cavity could raise the vorticity and promote the mixing. The effect of baffle's configurations on the mixing process was analyzed by comparing the flow properties, mixing efficiency, and total pressure loss. The baffle could induce large scale vortexes, promote the mixing layer to lose its stability easily, and then lead to the mixing efficiency enhancement. However, the baffle could increase the total pressure loss. The present investigation could provide guidance for applying new passive mixing enhancement methods for the supersonic mixing.

1. Introduction

High-speed flight vehicles call for new type propulsion system and scramjet has attracted researchers' attention to focus on this technique [1]. In order to adapt to the requirements of hypersonic vehicle at different flight Mach numbers, the dual combustor ramjet (DCR) was proposed, which was more superior to the conventional dual mode ramjet. The advantages include without fuel pretreatment, ignition and combustion stability, low Mach number launch, without mode conversion, and so on [2–4]. However, the superiority could result in complexity of the structure of engine and hence complicate internal flow and combustion characteristics. The combustion must occur quickly and requires fuel mix rapidly with oxidizer. In addition, the well mixing of fuel-rich gas from subsonic combustor with supersonic flow could achieve the advantages of DCR, and then the second combustion in supersonic combustor could proceed effectively. However, it is difficult to achieve the fully mixing of high-speed flows. Thus, the mixing enhancement measures to organize stable and efficient combustion in DCR are of importance.

The research on the mechanism of mixing layer contributes to perceive the flow stability, transition from laminar to turbulent and turbulence phenomena, finding the factors affecting the mixing efficiency. Initially, the study of the mixing layer was focused on the incompressible mixing layer, but the research on the compressible mixing layer has been carried out rapidly in recent decades under the promotion of the development of supersonic combustion technology [5–11]. Researchers usually use flow stability theory to theoretically analyze mixing layers [12–15] and find that the characteristics of compressible mixing layer changes with the increasing of convective Mach number. The mixing layer at low convective Mach number ($M_c < 0.4$) mainly preserves the two-dimensional instability, which is similar to the incompressible mixing layer, namely, the Kelvin-Helmholtz (K-H) instability [16]. K-H wave appears and enlarges gradually downstream, forming spanwise vortex structures (Brown-Roshko structure [17]) and then exhibits a certain three-dimensional feature. As M_c increases, the three-dimensional instability (Görtler instability [18]) becomes increasingly evident and the flow field becomes more disordered. In this case,

a significant characteristic is the streamwise vortex structure, embodying the three-dimensional characteristic. When M_c is greater than 0.6, the three-dimensional instability could possess the dominant position.

The numerical strategy has been an effective research method on the supersonic mixing layer, which has advantages such as flexibility, efficiency, and low cost. The numerical simulation could not only implement many conditions that experiments achieve difficultly but also provide details which experiments observe hardly. Numerical simulation could offer a valid, accurate numerical method and analytical tool for the research. However, the validation and trustworthiness will require proper models to simulate the turbulence and shock-vortex interaction. Reynolds-averaged Navier-Stokes (RANS) models, mainly used in engineering, are short for their prediction of the transient behavior. Large eddy simulation (LES) is most likely to be a realistic process for its time accurate feature [19]. However, the high order numerical schemes and adaptive subgrid model are required for the application of LES on such complex flows in compressible conditions. The numerical algorithms used in the resolution of supersonic flows play an essential role to achieve the accuracy of simulations. Flow discontinuities or the needs for shock-capture require higher order schemes, which, on the other hand, have poor behavior in turbulent regions and cost a large amount of computation time. Hybrid scheme combines the algorithms for the flow smoothness and discontinuities in one numerical scheme [20, 21]. In the present paper, a hybrid compact-WENO scheme, which deals with the smooth regions with compact scheme and uses WENO scheme to achieve the shock-capturing capability, is applied. Another focus about the feasibility of the application of LES on supersonic flows is the subgrid closure models. However, many models are based on incompressible closures and the development of subgrid models for compressible flow is limited.

The feasible mixing mechanisms exist in the scramjet flow field including parallel streams and nonparallel streams. The former loses little total pressure, but it needs a long distance to mix completely at the molecular level, resulting in a large size combustor. On the other hand, the latter jets fuel vertically to the gas stream, causing the fuel enters the air rapidly and forming convection significantly, which accompanies with three-dimensional effects, such as swirling motion. Thus this method could finish mixing process in a short distance. However, it could generate shock waves, resulting in considerable loss of momentum and total pressure. With an increase of M_c, the mixing layer becomes more stable and the growth rate is inhibited. Therefore, the enhancement measures are needed. Generally, these measures are divided into passive excitation, active excitation, three-dimensional jets, and generation of streamwise vortices [22–25]. The passive excitation makes the mixing layer lose its stability mainly by changing the physical configuration in the flow field and typical mixing devices include ramps, tabs, lobe mixers, and cavities [26–28]. The active excitation introduces incentive methods to destabilize the mixing layer and improve its growth rate. Vibrating splitter, Helmholtz resonators, piezoelectric actuators, and acoustic excitation are common devices for the active excitation [24]. Most of the measures' aim is to generate large scale structures and streamwise vortices attracted much attention [29–35]. Large-scale streamwise vortices are passively formed and the instability of mixing layer is excited, usually applying injections from struts of trailing ramp with different configurations.

Mixing of fuel with air at minimum pressure loss level is the idealist situation and the mixing of parallel streams meets this target. In this paper, mixing of parallel streams (M_c = 0.2) under the effect of baffles with different configurations was studied and this effect on the mixing enhancement was then analyzed.

TABLE 1: Flow parameters of supersonic mixing layer.

Inlet no.	Velocity (ms^{-1}) U_1, U_2	Ma Ma$_1$, Ma$_2$	Density (kgm^{-3}) ρ_1, ρ_2	Pressure (kPa) P_1, P_2	M_c
1	519	2.04	1.0	46	0.20
2	409	1.4	0.76		

2. Physical Model and Numerical Scheme

2.1. Physical Model.
Considered the supersonic mixing layer in supersonic combustor of DCR, the calculation domain and boundary conditions were shown in Figure 1.

The flow parameters were chosen to be the same as case 1 in [36], as shown in Table 1.

The separated flow could result in large scale structures and the separation could be caused by a sudden compression mainly due to the change in geometry, such as a forward-facing step or a backward-facing step. We utilized these configurations to disturb the flow and detect their influence on the mixing process. Baffles of different geometries, as shown in Table 2, were employed to achieve mixing enhancement. Then four cases were considered in the numerical simulations. Plates in four cases had the same width, which equaled 20 mm, and their sizes could be calculated with the aspect ratio, respectively. Besides, the development of free supersonic mixing layer without baffle (case 5) was added as the reference case.
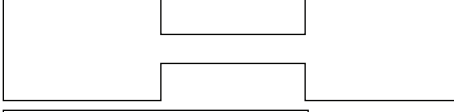
2.2. Governing Equations.
Applying the Deardorff box filtering, unsteady compressible Navier-Stokes equations, regardless of body force and external heat source, were written in the Cartesian coordinate system as follows:

$$\frac{\partial \overline{\rho}}{\partial t} + \frac{\partial \overline{\rho}\widetilde{u}_j}{\partial x_j} = 0, \tag{1}$$

$$\frac{\partial \overline{\rho}\widetilde{u}_i}{\partial t} + \frac{\partial \left(\overline{\rho}\widetilde{u}_i\widetilde{u}_j + \overline{P}\delta_{ij} - \overline{\tau}_{ij} + \tau_{ij}^{\mathrm{sgs}} \right)}{\partial x_j} = 0, \tag{2}$$

$$\frac{\partial \overline{\rho}\widetilde{E}}{\partial t} + \frac{\partial \left[\left(\overline{\rho}\widetilde{E} + \overline{P} \right) \widetilde{u}_j - \widetilde{u}_k\overline{\tau}_{kj} + \overline{q}_j + q_j^{\mathrm{sgs}} \right]}{\partial x_j} = 0, \tag{3}$$

TABLE 2: Baffles' configurations and sizes.

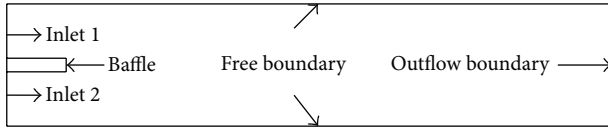| Case no.	Baffle type	Configuration schematic diagram	Size description
Case 1	Rectangular plate		Aspect ratio: 4 : 1
Case 2	Protruding plate		Protruding plate's aspect ratio: 4 : 1
Case 3	Symmetric cavity plate		Cavities' aspect ratio: 4 : 1
Case 4	Asymmetric cavity plate		Cavities' aspect ratio: 4 : 1
Case 5	—	—	—

FIGURE 1: Schematic diagram of computational model.

$$\overline{\tau}_{ij} = \mu \left(\frac{\partial \overline{u}_i}{\partial x_j} + \frac{\partial \overline{u}_j}{\partial x_i} - \frac{2}{3} \frac{\partial \overline{u}_k}{\partial x_k} \delta_{ij} \right), \qquad \overline{q}_j = k_f \frac{\partial \overline{T}}{\partial x_j}. \tag{4}$$

Equations (1)–(3) were the mass, momentum, and total energy conservation equations, respectively. The ideal gas state equation was needed to close the above equations:

$$\overline{P} = \overline{\rho} \widetilde{R} \widetilde{T}. \tag{5}$$

The Smagorinsky subgrid scale model was employed:

$$\tau_{ij}^{\text{sgs}} = \left(\overline{u_i} \overline{u_j} - \overline{u_i u_j} \right) = 2 (C_s \Delta)^2 \overline{S}_{ij} \left(2 \overline{S}_{ij} \overline{S}_{ij} \right)^{1/2} - \frac{1}{3} \overline{\tau}_{kk} \delta_{ij}, \tag{6}$$

$$q_j^{\text{sgs}} = - \frac{C_s \overline{\rho} \Delta^2 \sqrt{2 \overline{S}_{ij} \overline{S}_{ij}}}{\text{Pr}} \frac{\partial \overline{T}}{\partial x_j}.$$

The passive scalar f was introduced to present the transportation process and it did not affect other conserved quantity. The governing equation, ignoring subgrid convective and diffusive fluxes, was read as

$$\frac{\partial \overline{\rho} \widetilde{f}}{\partial t} + \frac{\partial \left[\overline{\rho} \widetilde{u}_j \widetilde{f} - \overline{\rho} \overline{D} \left(\partial \widetilde{f} / \partial x_i \right) \right]}{\partial x_j} = 0. \tag{7}$$

D was the mass diffusion coefficient of passive scalar.

Quantitative evaluations of the mixing characteristics were the mixing layer thickness and mixing efficiency.
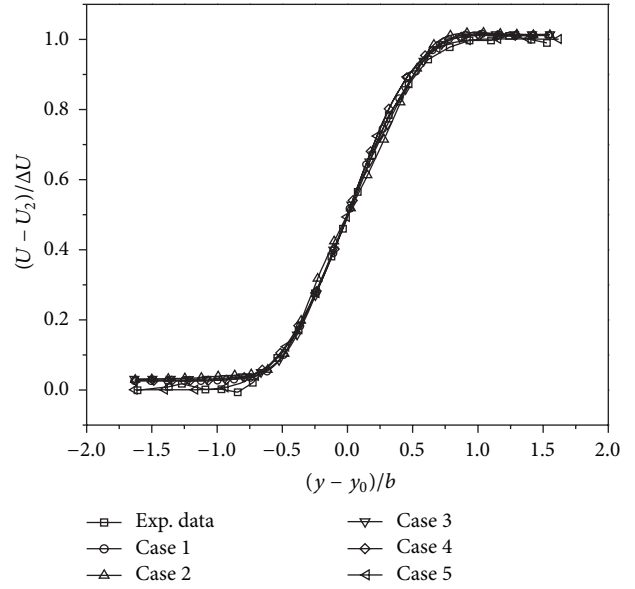
FIGURE 2: Mean velocity similarity profiles of $(U - U_2)/\Delta U$ at $0.9L_x$.

The mixing layer thickness represented the amount of free fluid entrained in the mixing layer, reflecting the strength of mixing, and mixing efficiency evaluated the mixing level. Here the mixing efficiency suggested by Lu and Wu [37] was applied:

$$\varepsilon_m (x) = \frac{4 \int_0^x \int_y \overline{\rho^2 f (1 - f)} dy \, d\xi}{\int_0^x \int_y \overline{\rho^2} dy \, d\xi}. \tag{8}$$

$\varepsilon_m(x)$ indicated the mixed fluid's proportion of the total amount of fluid from the inlet to the position x. The mixing efficiency became 1 when the passive scalars of whole fluid were 0.5, signifying that fluids were fully mixed.
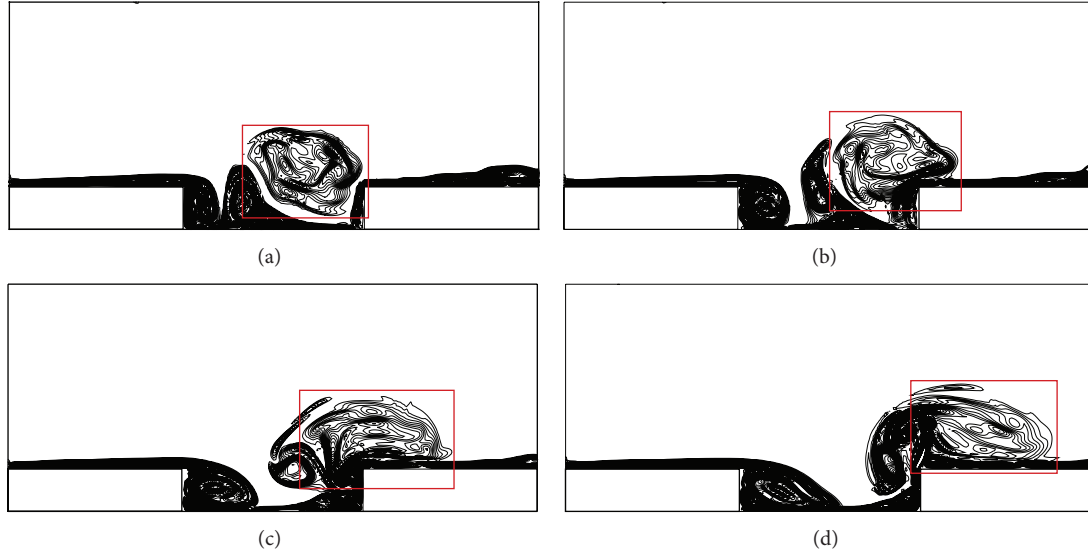
(a)

(b)

(c)

(d)

FIGURE 3: Instantaneous vorticity contours at four different times during the period of vortex-rear wall interaction.

2.3. Numerical Methods. Simulations of supersonic flows need high-resolution and high-precision numerical schemes for capturing the tiny flow structures in the complex flow field. Hence, in this paper a hybrid compact-WENO scheme proposed by Ren et al. [38] was applied to discretize the convective terms, obtaining the nonviscous flux, and a sixth-order symmetric compact difference scheme was used for the viscous diffusion terms. An explicit third-order Runge-Kutta method was used for the time integration.

Top and bottom boundaries were set as infinity, for artificially simulating a free mixing layer, so that the boundary conditions did not affect the internal flow fields. Besides, an immersed boundary method [39] was used to construct the baffle configurations.

Since the supersonic mixing layer has inherent stability and expands very slow, considering the development of mixing layer without the effect of baffles, the streamwise distance should be long enough for the vortex rolling-up and pairing. Hence, the computational domain is taken as a rectangular area ($L_x = 1.2$ m, $L_y = 0.2$ m) and discretized with 512×259 grid cells after a grid-independent verification.

3. Results and Discussions

3.1. Code Validation. When the mixing layer flow is fully developed, the statistics of flow field preserve the self-similarity. The mean streamwise velocity was compared for the five cases and the similarity coordinate used $\eta = (y - y_0)/b$. To compare the results of mixing layer's development, the profile at $x = 0.9L_x$ was shown for each case.

Figure 2 shows the dimensionless mean streamwise velocity in a similarity coordinate. Compared with the experiment data [36], it is shown that each case preserves a good self-similarity. The curves of five cases almost overlap, indicating that they all have been fully developed at $0.9L_x$ and the size of the computational domain is suitable. Hence, our

numerical method is validated for the further study of the baffle's effect on the supersonic mixing process.

3.2. Supersonic Cavity Flow Features. The cavity configuration contributes to induce large scale vortex and its relation with the mixing efficiency enhancement should be studied firstly. The mechanism of the effect on the mixing enhancement is not only relevant to the cavity shear layer but also governed by the disturbance from the cavity self-oscillation. Large scale structures influence the mixing process. Furthermore, the size of large scale vortex increases when the Mach number of free stream deceases. In order to distinctly observe the behavior of large scale structure, a supersonic flow with 1.2 Mach passing a cavity with length-to-depth ratio that equaled 4 was simulated. Figure 3 shows that the cavity flow is characterized by the large scale vortex shedding, whose spatial scale has a dimension of nearly the cavity size. When this large vortex is forming and moving downstream inside the cavity, the free mainstream is entrained into the cavity. As the large vortex impacts on the rear wall, it causes the flow seperation, forming a relatively large vortex and several smaller vortexes. The impingement process is a violent event, resulting in a large rise of vorticity, as shown in Figure 4. The rising of vorticity could let the irrotational free-stream fluid rotate into the vortex, and thus the mixing is enhanced. The large vortex, separated by the impingement, moves downstream and participates in the following mixing process. Hence, the large size vortexes formed in the cavity configuration could result in promoting the mixing efficiency.

3.3. Numerical Results. The large eddy coherent structure is an important feature of supersonic plane mixing layer, and the spanwise vorticity controls the development of the mixing layer.

Figure 5 shows the contours of vorticity, from which the large structures could be easily identified in flow field for
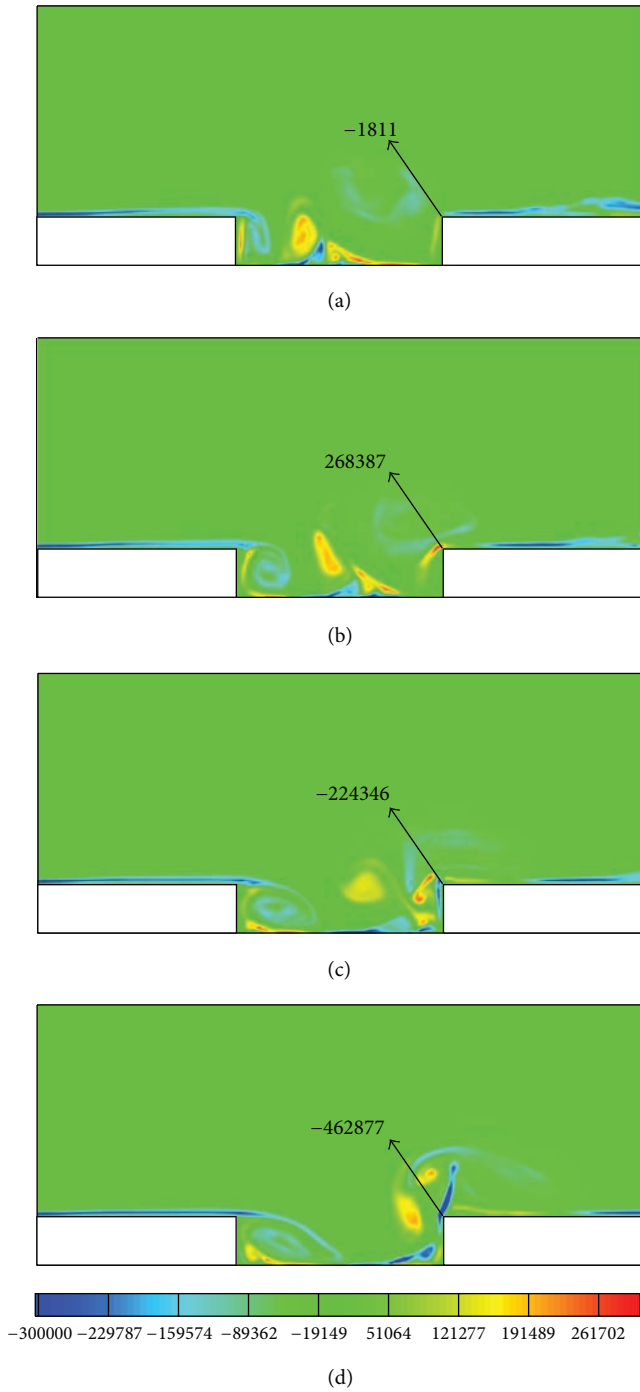
(a)

(b)

(c)

(d)

FIGURE 4: Variation of vorticity near trailing edge during the period of vortex-rear wall interaction.

(a)

(b)

(c)

(d)

(e)

FIGURE 5: Instantaneous vorticity contours in mixing layers (from top to bottom: case 1–case 5).

the cases with baffles. Generally, the flow loses its stability at the upstream when the fluid departs from the recirculation regions after baffles. Then the mixing layer grows through the rolling up, pairing, and shedding of vortices, often achieved by the interaction of two neighboring vortices.

The large scale structures in the wake region of the baffles contribute to enhance the mixing process. The present research results show that the mixing layer with high M_c
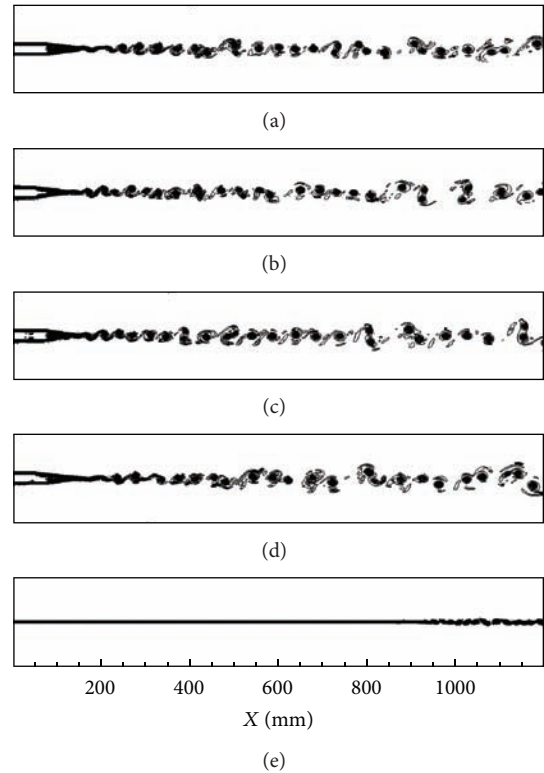
is much more stable and develops slowly, with large vortex unclearly being observed. In case 5, although the outlet streamwise velocity profile satisfies the self-similarity, much longer distance is needed for the vortex to roll up and the vortex structures are much more smaller, compared with the cases with baffles.

Figure 6 shows the instantaneous scalar contours of five cases at the same instant. Under the effect of cavities, large scale eddies appear in the mixing layer of case 3 and case 4. Inside the cavity there exists recirculation zone with low speed, generating a shear layer between this zone and the mainstream due to the speed difference. The mixing enhancement mechanism of baffles with cavities may relate to two factors: one is the function of the shear layer of cavity; the other is the periodic disturbance with a certain spectral characteristics aroused by cavity self-oscillation. Furthermore, the vorticity structures in case 3 appear more orderly than those of case 4 and it contributes to the stabilization of the flow. Therefore, the cavity structure could be more effective than convex structure. In addition, the range of recirculation region in case 2 is smaller than the other cases (not including case 5) due to the protruding configuration, resulting in smaller scale of vortex structures. Without baffles, the flow starts rolling up eddies downward at a long distance from the inlet in case 5. It is seen that baffles could significantly increase the mixing layer thickness from the time-averaged scalar distribution, displayed in Figure 7. The mixing layer thickness of case 3 is slightly larger than the other cases and
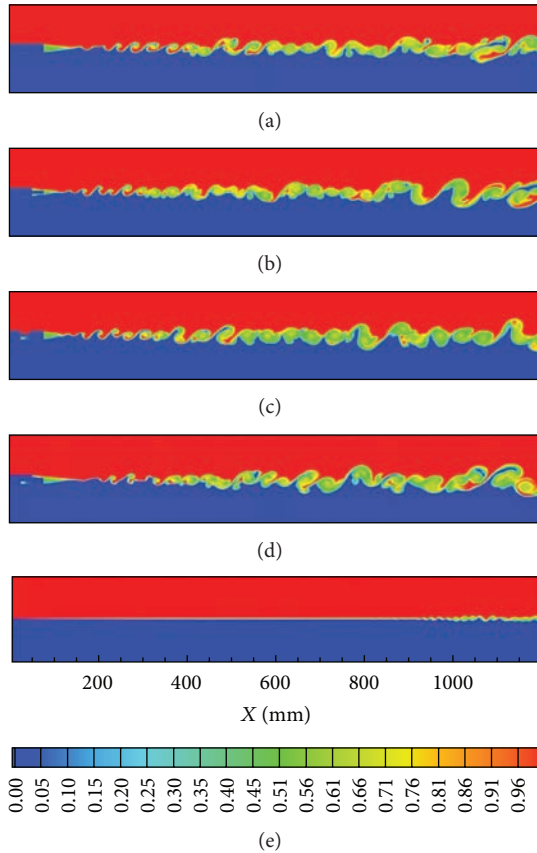
(a)

(b)

(c)

(d)

(e)

FIGURE 6: Instantaneous scalar contours in mixing layers (from top to bottom: case 1–case 5).

(a)

(b)

(c)

(d)

(e)

FIGURE 7: Time-averaged scalar contours in mixing layers (from top to bottom: case 1–case 5).

case 4 is larger than the first two cases, indicating that the cavity configurations on baffles help to promote the mixing process. The situation of protruding configuration (case 2) is nearly the same as the rectangle configuration (case 1). Their mixing layer thicknesses are almost the same near the exit of the computational domain, but there exists a difference during the developing procedure of mixing layer thickness.

Figure 8 shows the comparison of the mixing efficiency. ε_m of each case increases downstream, however, in different growth rates. ε_m of case 3 is larger than others along the flow direction. There is difference between case 2 and case 4 at the initial stage, but it disappears at the end of computational domain. The scalar contours in Figure 5 display that the first four cases have almost the same mixing layer thickness. Nevertheless, the curve of mixing efficiency clearly exhibits the difference. Mixing efficiency could be decided by the level of vortex spatial scale. If the vortex spatial scale is relatively small, the fluid in mixing layer will contain more tiny structures, enlarging the contact area between the fluids entrained in the mixing layer, and then it is beneficial for the mixing. Besides, ε_m of the cases with baffles is significantly better than case 5, demonstrating the effectiveness of baffles.

Reynolds stress is much larger than viscous stress in turbulent mixing, which represents the transverse transportation of streamwise momentum. Figure 9 shows the Reynolds stress at different streamwise sections for the first
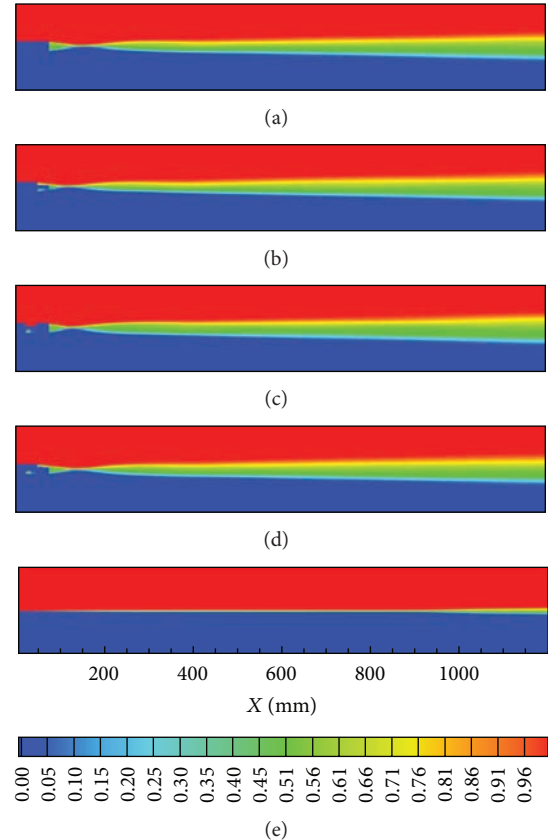
four cases. Reynolds stress has a large value in the center area of mixing layer. It could have significant effects on the growth rates of mixing layer and mixing efficiency. In case 3, this stress seems like decreasing downstream from $0.6L_x$; however, it is still larger than others for the first two profiles, showing a large amount of transverse transportation. This could be matched in Figure 6 and the slope of curve for case 3 decreases from $0.6L_x$. Besides, Reynolds stress of case 1 has a same decreasing trend and it corresponds with its curve of mixing efficiency. Reynolds stress in case 2 keeps approximately constant from $0.6L_x$ to $0.8L_x$ and then drops by 50 percent at $0.9L_x$. The opposite situation appears in case 4, with a rising at $0.8L_x$ and then keeps stable. Since the flow status after baffles is complex and the development of Reynolds stress is relatively disorder, it requires more detailed research.

The variation of total pressure significantly affects the combustor performance. The characteristics of total pressure are studied in the mixing layers. Figure 10 displays the development of total pressure loss downstream. Cases with baffles exhibit similar trends: the total pressure loss increases due to the compression waves generated by the reduction of flow passage, reaches to the peak, and then drops under the impact of expansion waves caused by the expansion of flow passage. Then, total pressure loss rises initially since the initial development of the mixing layer and the vortex begin
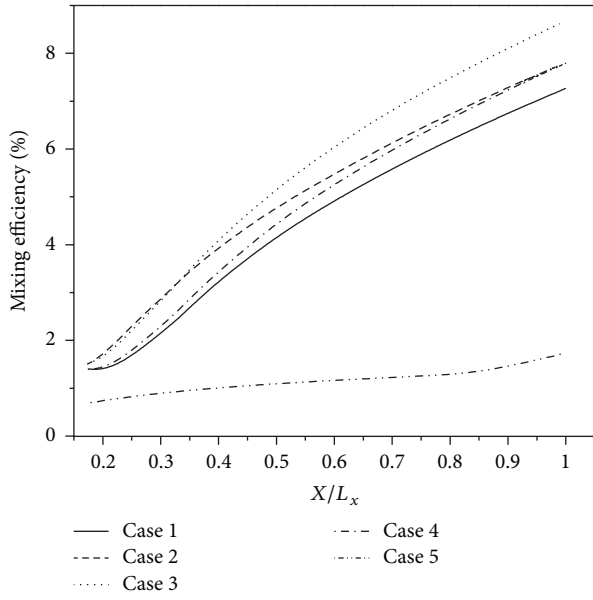
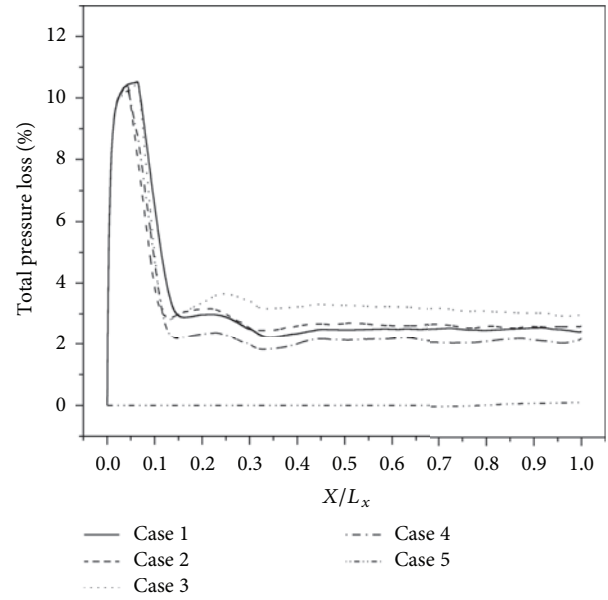FIGURE 8: Development of mixing efficiency for five cases.
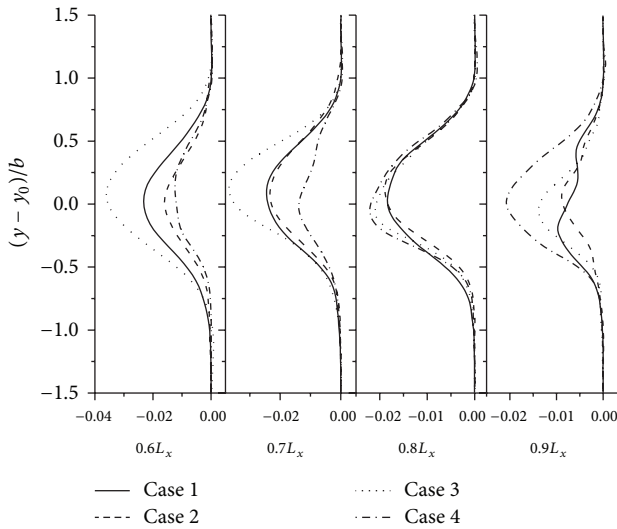

FIGURE 10: Development of total pressure loss.

FIGURE 9: Development of normalized Reynolds stress $u'v'/(\Delta U)^2$.

expansion waves by the configuration of baffles suitably will lead to a satisfactory mixing behavior and minimize the total pressure loss.

4. Conclusions

A LES numerical method coupled with immersed boundary method was applied to study the mixing characteristics of supersonic mixing layer, and especially the baffle configuration's influences on the mixing were analyzed. The results show that the entire development process of mixing layer experiences three stages of laminar, transition, and turbulent flow in turn. The molecular diffusion dominates in the laminar flow. Large-scale structures control the transition status and the fully turbulent region.

(1) The simulation results of the supersonic cavity flow illustrate large scale vortexes form inside the cavity and there appears a rise of vorticity after large scale vortexes' impingement on the rear wall. The separated vortexes could participate in the subsequent mixing and the increase of vorticity could result in the mixing enhancement.

(2) Baffles have an effect on the mixing enhancement. Large-scale structures in the wake regions behind the baffle and the compression waves in the leading edge of baffles could enhance the mixing. In addition, the rear region in the cavities of the baffle stabilized the mixing layer. The cavity, which configuration combines a forward-facing step and a backward-facing step, has a better performance on promoting the mixing efficiency.

(3) The introduction of baffles could result in choked flow and increase total pressure loss. Although cavity plates could bring in a large total pressure loss,

to roll up, and then this value keeps nearly stable after a slight decrease, indicating that the mixing layer has been fully developed. On the other hand, total pressure loss of case 5 keeps steady for a long distance until almost 900 mm and then ascends slightly, showing the development of mixing layer. Obviously, instability and development of mixing layer could increase the total pressure loss. The smaller the flow passage changes, the stronger the compression waves form and the larger the total pressure loss is reached; therefore the top value of case 1 and 3 is larger than others. Compared with Figure 6, the general trend is that well mixing combines with large total pressure loss. Particularly, case 1 loses more total pressure than case 4. However, 4 mixes better than case 1. This phenomenon may illustrate that inducing compression and

their effective influence on the mixing process will provide useful information for the mixing of fuel and oxidizer in the supersonic chamber. Furthermore, the proper location of cavities on the baffle could provide appropriate mixing characteristics and reduce the total pressure loss.

Conflict of Interests

The authors declare that they have no financial and personal relationships with other people or organizations that can inappropriately influence their work. There is no professional or other personal interest of any nature or kind in any product, service, and/or company that could be construed as influencing the position presented in, or the review of the paper.

Acknowledgments

References

[1] J. M. Tishkoff, J. P. Drummond, T. Edwards et al., "Future directions of supersonic combustion research—air force/NASA workshop on supersonic combustion," AIAA Paper 97-1017, 1997.

[2] F. S. Billig, P. J. Waltrup, and R. D. Stockbridge, "Integral-rocket dual-combustion ramjets: a new propulsion concept," *Journal of Spacecraft and Rockets*, vol. 17, no. 5, pp. 416–724, 1980.

[3] J. L. Keirsey, "Airbreathing propulsion for defense of the surface fleet," *Johns Hopkins APL Technical Digest*, vol. 13, no. 1, pp. 57–68, 1992.

[4] E. T. Curran, "Scramjet engines: the first forty years," *Journal of Propulsion and Power*, vol. 17, no. 6, pp. 1138–1148, 2001.

[5] D. Papamoschou and A. Roshko, "Compressible turbulent shear layer: an experimental study," *Journal of Fluid Mechanics*, vol. 197, pp. 453–477, 1988.

[6] D. Papamoschou, "Structure of the compressible turbulent shear layer," AIAA Paper 89-0126, 1989.

[7] T. L. Jackson and C. E. Grosch, "Inviscid spatial stability of a compressible mixing layer," *Journal of Fluid Mechanics*, vol. 208, pp. 609–637, 1989.

[8] G. S. Elliott and M. Samimy, "Compressibility effects in free shear layers," *Physics of Fluids A*, vol. 2, no. 7, pp. 1231–1240, 1990.

[9] G. S. Elliott, M. Samimy, and S. A. Arnette, "The characteristics and evolution of large-scale structures in compressible mixing layers," *Physics of Fluids*, vol. 7, no. 4, pp. 864–876, 1995.

[10] A. W. Vreman, N. D. Sandham, and K. H. Luo, "Compressible mixing layer growth rate and turbulence characteristics," *Journal of Fluid Mechanics*, vol. 320, pp. 235–258, 1996.

[11] J. B. Freund, S. K. Lele, and P. Moin, "Compressibility effects in a turbulent annular mixing layer. Part 1. Turbulence and growth rate," *Journal of Fluid Mechanics*, vol. 421, pp. 229–267, 2000.

[12] P. Huerre and P. A. Monkewitz, "Absolute and convective instabilities in free shear layers," *Journal of Fluid Mechanics*, vol. 159, pp. 151–168, 1985.

[13] T. L. Jackson and C. E. Grosch, "Absolute/convective instabilities and the convective Mach number in a compressible mixing layer," *Physics of Fluids A*, vol. 2, no. 6, pp. 949–954, 1990.

[14] O. Peroomian and R. E. Kelly, "Absolute and convective instabilities in compressible confined mixing layers," *Physics of Fluids*, vol. 6, no. 9, pp. 3192–3194, 1994.

[15] L.-S. Lee and P. J. Morrist, "Absolute instability in a supersonic shear layer and mixing control," *Journal of Propulsion and Power*, vol. 13, no. 6, pp. 763–767, 1997.

[16] L. P. Bernal and A. Roshko, "Streamwise vortex structure in plane mixing layers," *Journal of Fluid Mechanics*, vol. 170, pp. 499–525, 1986.

[17] G. L. Brown and A. Roshko, "On density effects and large structure in turbulent mixing layers," *Journal of Fluid Mechanics*, vol. 64, no. 4, pp. 775–816, 1974.

[18] H. Görtler, "On the three-dimensional instability of laminar boundary layers on concave walls," NACA TM 1375, 1954.

[19] F. Génin and S. Menon, "Simulation of turbulent mixing behind a strut injector in supersonic flow," *AIAA Journal*, vol. 48, no. 3, pp. 526–539, 2010.

[20] N. A. Adams and K. Shariff, "A high-resolution hybrid compact-eno scheme for shock-turbulence interaction problems," *Journal of Computational Physics*, vol. 127, no. 1, pp. 27–51, 1996.

[21] S. Pirozzoli, "Conservative hybrid compact-WENO schemes for shock-turbulence interaction," *Journal of Computational Physics*, vol. 178, no. 1, pp. 81–117, 2002.

[22] E. J. Gutmark, K. C. Schadow, and K. H. Yu, "Mixing enhancement in supersonic free shear flows," *Annual Review of Fluid Mechanics*, vol. 27, no. 1, pp. 375–417, 1995.

[23] D. M. Bushnell, "Hypervelocity scramjet mixing enhancement," *Journal of Propulsion and Power*, vol. 11, no. 5, pp. 1088–1090, 1995.

[24] J. M. Seiner, S. M. Dash, and D. C. Kenzakowski, "Historical survey on enhanced mixing in scramjet engines," *Journal of Propulsion and Power*, vol. 17, no. 6, pp. 1273–1286, 2001.

[25] V. A. Vinogradov, Y. M. Shikhman, and C. Segal, "A review of fuel pre-injection in supersonic, chemically reacting flows," *Applied Mechanics Reviews*, vol. 60, no. 1–6, pp. 139–148, 2007.

[26] S. Sujith, T. M. Muruganandam, and J. Kurian, "Effect of trailing ramp angles in strut-based injection in supersonic flow," *Journal of Propulsion and Power*, vol. 29, no. 1, pp. 66–78, 2013.

[27] P. Behrouzi and J. J. McGuirk, "Effect of tabs on rectangular jet plume development," *Journal of Propulsion and Power*, vol. 25, no. 4, pp. 930–939, 2009.

[28] D. P. Mishra and K. V. Sridhar, "Numerical study of effect of fuel injection angle on the performance of a 2D supersonic cavity combustor," *Journal of Aerospace Engineering*, vol. 25, no. 2, pp. 161–167, 2012.

[29] E. M. Fernando and S. Menon, "Mixing enhancement in compressible mixing layers: an experimental study," *AIAA Journal*, vol. 31, no. 2, pp. 278–285, 1993.

[30] T. Sunami, M. N. Wendt, and M. Nishioka, "Supersonic mixing and combustion control using streamwise vortices," AIAA Paper 98-3271, 1998.

[31] C. J. Bourdon and J. C. Dutton, "Mixing enhancement in compressible base flows via generation of streamwise vorticity," *AIAA Journal*, vol. 39, no. 8, pp. 1633–1635, 2001.

[32] M. Kodera, T. Sunami, and F. Scheel, "Numerical study on the supersonic mixing enhancement using streamwise vortices," AIAA Paper 2002-5117, 2002.

[33] S. Watanabe and M. G. Mungal, "Velocity fields in mixing-enhanced compressible shear layers," *Journal of Fluid Mechanics*, vol. 522, pp. 141–177, 2005.

[34] N. Chauvet, S. Deck, and L. Jacquin, "Numerical study of mixing enhancement in a supersonic round jet," *AIAA Journal*, vol. 45, no. 7, pp. 1675–1687, 2007.

[35] S. Sujith, T. M. Muruganandam, and J. Kurian, "Effect of trailing ramp angles in strut-based injection in supersonic flow," *Journal of Propulsion and Power*, vol. 29, no. 1, pp. 66–78, 2013.

[36] S. G. Goebel, J. C. Dutton, H. Krier, and J. P. Renie, "Mean and turbulent velocity measurements of supersonic mixing layers," *Experiments in Fluids*, vol. 8, no. 5, pp. 263–272, 1990.

[37] P. J. Lu and K. C. Wu, "On the shock enhancement of confined supersonic mixing flows," *Physics of Fluids A*, vol. 3, no. 12, pp. 3046–3062, 1991.

[38] Y.-X. Ren, M. Liu, and H. Zhang, "A characteristic-wise hybrid compact-WENO scheme for solving hyperbolic conservation laws," *Journal of Computational Physics*, vol. 192, no. 2, pp. 365–386, 2003.

[39] C. S. Peskin, "Flow patterns around heart valves: a numerical method," *Journal of Computational Physics*, vol. 10, no. 2, pp. 252–271, 1972.